water [logo]

MDPI

Article

Biochar from A Freshwater Macroalga as A Potential Biosorbent for Wastewater Treatment

Izabela Michalak [1],*, Sylwia Baśladyńska [1], Jakub Mokrzycki [2] and Piotr Rutkowski [2]

[1] Department of Advanced Material Technologies, Faculty of Chemistry, Wrocław University of Science and Technology, Smoluchowskiego 25, 50-372 Wrocław, Poland

[2] Department of Polymer and Carbonaceous Materials, Faculty of Chemistry, Wrocław University of Science and Technology, Wybrzeże Wyspiańskiego 27, 50-370 Wrocław, Poland

* Correspondence: izabela.michalak@pwr.edu.pl; Tel.: +48-71-320-2434

[check for updates]

Abstract: The multi-elemental composition, surface texture and morphology of biochar, produced by pyrolysis at 300, 350, 400 and 450 °C from freshwater macroalga *Cladophora glomerata*, as a biosorbent of toxic metals was examined with Inductively Coupled Plasma Optical Emission Spectrometry (ICP-OES), Scanning Electron Microscopy (SEM), and Fourier Transform Infrared Spectroscopy (FT-IR) techniques. It was found that the yield of pyrolysis was inversely proportional to temperature: for 300 °C it was 63%, whereas for 450 °C—47%. The proximate analysis revealed that also biochar's moisture and volatile matter was inversely proportional to temperature. The content of ash increased with temperature. All biochars were characterized by a similar total pore area of about 20 m^2 g^{-1}. FT-IR analysis showed that all biochars peaked at 3500–3100 cm^{-1} which was attributed to O–H stretching of the hydroxyl groups, at 2850–2970 cm^{-1}, stretching vibrations of C–H bonds in aliphatic CH_2 and CH groups, at 1605 cm^{-1}, stretching vibrations from C=C of aromatics, at 1420 cm^{-1}, bending oscillations from CH_2, at about 1111 cm^{-1}, stretching vibrations of Si–O, at 618 cm^{-1}, vibrations from Fe–O bonds, and at 475 cm^{-1}—Si–O–Si deformation vibrations. The biosorption properties of biochar towards Cr(III) ions were examined in kinetic studies. The biosorption capacity of biochar increased with an increase of pyrolysis temperature: the highest was for biochar obtained at 450 °C—87.1 mg Cr(III) g^{-1} and the lowest at 300 °C—45.9 mg g^{-1}. *Cladophora* biochar also demonstrated a good ability to simultaneously remove metal ions from a multi-metal system, e.g., wastewater. The removal efficiency for Cr(III) was 89.9%, for Cu(II) 97.1% and for Zn(II) 93.7%. The biochar derived from waste-freshwater macroalgae can be a potent and eco-friendly alternative adsorptive material.

Keywords: *Cladophora glomerata*; biochar; characteristics; biosorption; wastewater treatment; Cr(III) ions

1. Introduction

Marine and freshwater macroalgae provide essential ecosystem services and biomass for different applications [1]. They constitute a valuable source of biologically active compounds that can be used for the production of pharmaceuticals (chemicals), nutraceuticals, cosmetics, food, feed, fertilizers/biostimulants, etc. The downside is that the waste generated during their processing plus the natural occurrence of invasive species pose a major environmental problem [1–3]. One of the solutions to manage abounding green tide algae is pyrolysis, which is a thermal decomposition of biomass under oxygen-limited conditions, typically at a temperature range within 300–700 °C, within which algal waste can be converted to a solid product such as biochar, liquid (bio-oil) and gas [1,4–6]. This technique is relatively simple and inexpensive and allows considerable flexibility in both the type

and quality of the biomass feedstock [7]. For the production of biochar, mainly agricultural waste such as rice straw, wood and fruit peel and forestry waste are used as a feedstock [8–11]. The biomass of macroalgae (e.g., waste marine macroalgae: kelp [8,12]; *Undaria pinnatifida* [13]; *Saccharina japonica* and *Sargassum fusiforme* [6]; *Sargassum* sp. [14]; *Cladophora coelothrix*, *Cladophora patentiramea*, *Chaetomorpha indica*, *Chaetomorpha linum*, *Cladophoropsis* sp., *Ulva flexuosa* [1], as well as freshwater *Spirogyra* and *Cladophora* [4]; *Cladophora vagabunda* [1]; *Oedogonium intermedium* [15]) is increasingly proposed as a raw material for pyrolysis. The most recent publications concern marine macroalgae.

Algal biochar is characterized by a comparatively low carbon content, surface area and cation exchange capacity when compared with lignocellulosic biomass, but has a high pH plus nitrogen and inorganic nutrients such as Ca, K, Mg and P [1], which is why it is proposed to be used in agriculture as a soil fertilizer/soil additive. Its other applications include its use as an adsorbent for the removal of organic or inorganic pollutants or energy sources [1,5,12,14–16].

Algal biochar endowed with good biosorption properties is suitable for wastewater treatment like the removal of ammonium-N (NH_4^+-N) and various organic and inorganic pollutants from wastewaters [17]. Jung et al. (2016) used biochar for the sorption of phosphates [13], while Cole et al. (2017)—to recover dissolved nitrogen and phosphorous from municipal wastewater [15]. The biochar applied in this process was enriched with crucial macro-elements—N and P and can be incorporated into soil as a fertilizer additive [1,13,17].

The use of algal biochar as a biosorbent for the removal of toxic metals from wastewater should be studied more extensively. Alongside with chemical precipitation, membrane filtration, electrochemical treatment technologies, sorption is frequently used for removing heavy metals from wastewater, especially when their concentrations are low and range from 1 to 100 mg L^{-1} [18]. The possibility of the production of "bio-ore" from the metal-loaded sorbent at the end of the process is very advantageous. Combustion of biochar after sorption enables the recovery of metals and energy accumulated in biomass. The sale of recovered elements is known as "phyto-mining" [19]. Algal biochar has already been tested as a sorbent of some heavy metals such as Cu, Cd and Zn ions from aqueous solutions [6,8]. Kidgell et al. (2014) used the biochar produced from freshwater macroalga *Oedogonium* to remove metal ions from the industrial effluent coming from a coal-fired power station [20]. Johansson et al. (2016) showed that biochar produced from *Gracilaria* and *Oedogonium*, which were treated with Fe before pyrolysis, have a high affinity also for oxyanions such as As, Mo and Se, which are difficult to remove through conventional techniques [21].

Freshwater macroalga *Cladophora glomerata*, which originates from eutrophication, underwent pyrolysis to produce biochar. The influence of pyrolysis temperature on biochar properties was tested. Several analytical techniques—SEM (Scanning Electron Microscopy); FT-IR (Fourier Transform Infrared Spectroscopy) and ICP-OES (Inductively Coupled Plasma Optical Emission Spectrometry) plus proximate analysis were used to examine moisture, ash, volatile matter; multi-elemental composition and biosorption properties in the single and multi-metal system.

2. Materials and Methods

2.1. Freshwater Macroalga

The biomass of freshwater macroalga *Cladophora glomerata*, identified by morphological characteristics according to the taxonomic literature for the area [22], was collected by hand from the surface of a pond—a part of a private property whose owner gave us permission to carry out the experiment—in the village of Tomaszówek (51°27′21″N, 20°07′43″E) in August 2016 (Figure 1). Then it was air-dried and milled in grinding mills (Retsch GM 300, Haan, Germany).

Figure 1. *Cladophora glomerata* on pond surface (**a**) and air-drying of freshwater macroalgae (**b**) (Photo: Izabela Michalak).

2.2. Pyrolysis of Freshwater Macroalgae

Pyrolysis—the thermochemical conversion of freshwater macroalgae into biochar—was carried out in a Carbolite electric heated furnace. At first, about 15 g of the sample was weighed and placed in a quartz boat, and then in a quartz tube located horizontally inside the furnace. The introduction of a nitrogen flow of 20 L h^{-1} ensured an inert atmosphere in the reactor. Temperatures stood at 300, 350, 400 and 450 °C; the heating rate was 10 °C min^{-1} and the residence time was one hour. Once the process ended, the samples were cooled in nitrogen flow down to room temperature, weighed to define the solid yield and stored in a polypropylene tank. Samples were named as A300, A350, A400 and A450, where the numbers refer to temperatures under which biochars were obtained.

2.3. Yield of Biochars

The resultant biochar was weighed and its yield (*Y*) was determined by Equation (1):

$$Y = \frac{mass_{after\ pyrolysis}}{mass_{before\ pyrolysis}} \times 100\% \tag{1}$$

The yield of biochars after pyrolysis is given in Table 1.

2.4. Biosorption of Biochars

For the biosorption experiments, biochar with a particle size lower than 500 μm was chosen (sieve analysis, Retsch, Haan, Germany). The biosorption properties of biochars obtained at the temperatures of 300, 350, 400 and 450 °C were tested in biosorption kinetics. Chromium(III) ions (as Cr(NO$_3$)$_3$·9H$_2$O) were chosen as a model ion, due to the simple spectrophotometric method of their determination in aqueous solutions [23]. Experiments were performed in Erlenmeyer flasks containing 200 mL of Cr(III) solution (C_0 300 mg L^{-1}—initial concentration of metal ions) at an agitating rate of 150 rpm and room temperature (~20 °C) for three hours. The biomass content (C_S) was 1 g L^{-1} and pH 5: at a pH higher than 5.5, Cr(III) ions precipitate as hydroxide as our previous experiments proved [24,25]. The pH of the solutions was adjusted with a 0.1 mol L^{-1} solution of NaOH/HCl with a pH meter, Mettler-Toledo (Seven Multi, Greifensee, Switzerland), equipped with an InLab413 electrode with compensation of temperature. Reagents Cr(NO$_3$)$_3$·9H$_2$O and NaOH, HCl were purchased from Avantor Performance Materials Poland S.A. (Gliwice, Poland). Solutions after biosorption were filtered through filter paper.

Algal biochar was also tested as a sorbent of toxic metals, such as Cu(II), Cr(III) and Zn(II) ions occurring in artificial wastewater. The initial metal ions concentration was assumed to be low (according to [18,26]) and equal to 0.5 mg L^{-1} for Cu(II) ions, 1 mg L^{-1} for Cr(III) and 4 mg L^{-1} for Zn(II) ions. The initial solution was prepared with inorganic salts: CuSO$_4$·5H$_2$O and ZnSO$_4$·7H$_2$O

(Avantor Performance Materials Poland S.A., Gliwice, Poland). To 200 mL of the solution, 0.2 g of biochar was added. The contact time was two hours (determined from the kinetic experiments). After biosorption, the solution was filtered. The solution before and after biosorption (in the latter case it was filtered) was examined with ICP-OES.

2.5. Analytical Techniques

2.5.1. Proximate Analysis

For each analysis approximately 1 ± 0.0001 g of biochar was weighed out. Prior to the analysis, the sample was grinded to a particle size of <0.4 mm. Proximate analysis of samples included moisture (M)—determined according to standard PN-EN ISO 18134-2:2017-03 [27]. Samples were weighed and held in the oven for 1.5 h at 105 °C ± 5 °C, until they reached constant mass. Ash (A)—was measured according to standard PN-ISO 1171 [28]. Samples were weighed and heated from ambient temperature up to 815 °C ± 10 °C and held for 1.5 h until constant mass was reached. Determination of the volatile matter (VM) was conducted according to standard PN-EN ISO 18123:2016-01 [29]. Samples were weighed and placed into the furnace heated to 850 °C ± 10 °C and held for seven minutes in the absence of air. Results are average values of two parallel measurements.

2.5.2. Surface Area Measurements

The surface area of biochar was determined with the Brunauer–Emmett–Teller (BET) method using a NOVA 2000 gas sorption analyser (Anton Paar QuantaTec Inc., Boynton Beach, FL, USA) for N_2 adsorption-desorption at 77 K. Pore volume distribution, bulk density and porosity of obtained biochars were evaluated with a mercury porosimeter (Micromertics AutoPore IV 9510, Micromeritics Instrument CORP, Norcross, GA, USA). Operating pressures were 0.1–400 MPa. Prior to the measurement, the samples were degassed under vacuum at 300 °C. About 0.1 g of the each biochar sample was used for the measurement.

2.5.3. Scanning Electron Microscopy (SEM) Analysis

SEM analyses were conducted with Scanning Electron Microscope—Jeol JSM-6610LVnx (JEOL USA Inc., Peabody, MA, USA) and the integrated system of an X-ray energy dispersive spectrometer (EDS) Oxford Aztec Energy. The operating accelerating voltage was 9 kV. The pressure range in the chamber in the low vacuum mode ranged from 10 Pa to 270 Pa.

2.5.4. FT-IR Analysis

Before analysis, samples of the natural biomass and obtained biochars were dried for 24 h at 80 °C. For FT-IR analysis, KBr discs were prepared with each containing 1.5 mg of the sample and 200 mg of KBr. The spectra were recorded on a Bruker spectrophotometer (Bruker FT-IR IFS 66/s; Billerica, MA, USA) in the mid IR range (4000–400 cm^{-1}).

2.5.5. Spectrophotometric Method

The concentration of Cr(III) ions in the solution before and after biosorption was determined spectrophotometrically at a wavelength of 540 nm. To 4 mL of the solution containing Cr(III) ions, 0.095 g EDTA (ethylenediaminetetraacetic acid, Avantor Performance Materials Poland S.A., Gliwice, Poland) was added. The sample was heated for 10 min at 95 °C. Cr(III) ions form violet complexes with EDTA. The Varian Cary 50 Conc. Instrument (Victoria, Australia) measured the absorbance of the samples. Detailed description of the methodology can be found in the work of Ni et al. (2002) [23] and Michalak and Chojnacka (2010) [24].

2.5.6. Multi-Elemental Composition

The analysis of the carbon content was performed with a Vario Macro Cube CN (carbon, nitrogen) analyser—(Elementar Analysensysteme GmbH, Langenselbold, Germany). The multi-elemental composition of the solutions before and after biosorption (for Zn(II) and Cu(II) ions) as well as tested biochars was determined with ICP-OES with a Varian VISTA-MPX ICP-OES spectrometer (Victoria, Australia) in the Chemical Laboratory of Multi-elemental Analysis, at Wrocław University of Science and Technology, accredited by the International Laboratory Accreditation Cooperation Mutual Recognition Arrangement and Polish Centre for Accreditation (No AB 696). Before the analysis, all samples of the biochar were digested with 5 mL of concentrated 69% HNO_3 (Supra pure grade from Merck, Darmstadt, Germany) in a microwave oven (type Milestone MLS-1200 MEGA, Bergamo, Italy). The solution after mineralization was diluted to 50 mL [24].

3. Results and Discussion

We performed the preliminary experiments on the biosorption of Cr(III) ions by *Cladophora glomerata* biochar in a single-metal system and Cr(III), Zn(II) and Cu(II) ions in a multi-metal system. First we dealt with the physical-chemical characterisation of the biochars. Proximate analysis determined moisture, ash and volatile matter. Mercury porosimetry defined the characteristics of the biochars (total intrusion volume, total pore area, apparent (skeletal) density, median pore diameter (area), average pore diameter, and porosity). Images from Scanning Electron Microscopy highlighted the internal structure of the biochars. Fourier Transform Infrared Spectroscopy determined functional groups that are responsible for metal ion biosorption. This characteristic decides about the potential applications of biochar. Available literature confirms that biochars produced from bio-waste, due to their properties—such as porous structure, high specific surface area and abundant functional groups, have been widely used to remove toxic metals from wastewater [6,8,12,14,30].

3.1. Yield of Algal Biochar and Its Proximate Analysis

The proximate analysis of a raw *Cladophora glomerata* and resultant biochars is given in Table 1.

Table 1. Proximate analysis of biochars (N = 2).

Sample	Moisture (M^a)	Ash (A^d)	Volatile matter (VM^{daf})	Yield of bio-char (Y)
	(wt.%)	(wt.%)	(wt.%)	(wt.%)
Cladophora glomerata	6.1 ± 0.1	19.7 ± 0.2	84.5 ± 0.8	-
A300	1.5 ± 0.0	30.3 ± 0.3	68.9 ± 0.7	63 ± 2
A350	1.7 ± 0.0	35.6 ± 0.4	60.1 ± 0.6	56 ± 1
A400	1.9 ± 0.0	39.1 ± 0.4	53.0 ± 0.5	50 ± 1
A450	1.5 ± 0.0	40.1 ± 0.4	50.0 ± 0.5	47 ± 1

a: analytical, d: dry basis, daf: dry, ash-free.

Cladophora glomerata is a typical aquatic biomass rich in mineral matter and a high part of volatile organics. As can be seen, applied thermal treatment parameters resulted in a drastic decrease in moisture content and increase in mineral matter. Biochars are characterized by a rather low amount of moisture that varies from 1.5 to 1.9 wt.%. The amount of ash varied within the range of 30–40 wt.% and is typical for such materials derived from algae [13]. The increase in the ash content with the increase in pyrolysis temperature is consistent with literature data. For instance, Jung et al. (2016) also observed this phenomenon for biochar produced at 200, 400, 600 and 800 °C from marine brown macroalga *Undaria pinnatifida* [13]. The ash content significantly increases with pyrolysis temperature mainly due to the minerals forming ash, which remain after biochar carbonization [30].

The rather low final temperature of pyrolysis leads to a partial removal of volatile matter. A high content of volatile matter within the samples is not only the result of the low temperature of pyrolysis,

but also the chemical composition of algae. Algae consist of proteins and mostly hemicellulose and cellulose [2]. The intensive decomposition of hemicellulose and cellulose during pyrolysis results in a high release of light hydrocarbons and their derivatives (acids, ketones), carbon monoxide and carbon dioxide. For the analysed samples, the VM content decreased along with the temperature rise from 84.5 wt.% to 50 wt.% for raw biomass and biochar A450, respectively. The same phenomenon was observed in the work of Chaiwong et al. (2012), who studied the proximate analysis of biochar obtained from *Cladophora* collected from the Nan River (Thailand) at 550 °C. The content of volatiles was lower in produced biochar (35.5%) than in raw macroalga (60.6%), whereas the content of carbon increased from 28.8% in *Cladophora* to 51.1% in biochar, as well as the ash content from 33.4% in *Cladophora* to 38.8% in biochar [4].

All these data are in line with the yield of biochars produced from freshwater macroalga, which at different temperatures of pyrolysis was as follows: 300 °C—63%, 350 °C—56%, 400 °C—50% and 450 °C—47%. A nearly linear decrease in solid residue formation occurred during thermal treatment of algae. A relatively high yield of biochar is a consequence of the medium temperature of the process, partial devolatilization and a high mineral matter content. It is a typical behaviour of such biomass materials. According to the review by Yu et al. (2017), the yield of biochar derived from macroalgae ranges from 8.1 to 62.4%, respectively (on a dry weight basis) [5]. Chaiwong et al. (2012) also produced biochar from freshwater *Cladophora glomerata* and the yield at 550 °C (higher than in the present study) was equal to 31% [4]. Our results correspond to the outcome presented by Poo et al. (2018), who produced biochars from brown seaweeds *Saccharina japonica* and *Sargassum fusiforme*. The higher temperature of pyrolysis—250, 400, 500, 600 and 700 °C was, the lower biochar yield—47.1, 37.3, 31.5, 29.7, 25.9% was received, respectively for *Saccharina japonica* and 58.4, 44.6, 38.3, 35.0 and 32.8%, respectively for *Sargassum fusiforme* [6]. Also, in the work of Jung et al. (2016) it was shown that an increase in pyrolysis temperature led to a decrease in the biochar yield produced from marine macroalga *Undaria pinnatifida* [13]. A higher yield indicates that the weight loss during pyrolysis is smaller, thus higher amounts of biochar can be obtained [6].

3.2. Mercury Porosimetry

Prior to biosorption tests, the surface area of all biochars was measured by means of N_2 sorption at 77 K and mercury porosimetry. The specific surface area (S_{BET}) of biochars was estimated to define textural properties, but no development of the microporosity during low-temperature thermal treatment of *Cladophora glomerata* was found. Therefore, mercury porosimetry was applied and its cumulative results are presented in Table 2.

Table 2. Porous texture data from mercury porosimetry (N = 2).

Sample	Total Intrusion Volume	Total Pore Area	Apparent (Skeletal) Density	Median Pore Diameter (Area)	Average Pore Diameter (4V/A)	Porosity
-	$cm^3 \ g^{-1}$	$m^2 \ g^{-1}$	$g \ cm^{-3}$	nm	nm	%
A300	0.557 ± 0.028	20 ± 1	1.64 ± 0.08	7.6 ± 0.2	110 ± 3	48 ± 2
A350	0.727 ± 0.036	19 ± 1	1.66 ± 0.08	7.7 ± 0.2	156 ± 4	55 ± 3
A400	0.806 ± 0.040	19 ± 1	1.54 ± 0.08	7.9 ± 0.2	166 ± 4	55 ± 3
A450	0.773 ± 0.039	21 ± 1	1.57 ± 0.08	7.3 ± 0.2	148 ± 4	55 ± 3

All biochar samples were characterized by rather small, but comparable total pore areas. The increase in pyrolysis temperature did not affect significantly the textural properties of the material and all samples had a total pore area of about 20 $m^2 \ g^{-1}$. Usually, with the increase in pyrolysis temperature, the specific surface area also increases, mainly due to the destruction of organic functional groups and formation of micro-pores in the produced biochars [30].

The total volume intrusion increased along with the temperature rise and varied from 0.557 cm^3 g^{-1} to about 0.806 cm^3 g^{-1}. Such a phenomenon might be related to a rather high amount of ash within the samples—mostly silica—thus the total pore area of the sample remained stable within the studied temperature range. The amount of ash varied from about 30 wt.% up to 40 wt.% (dry basis). All samples were characterized by a comparable median pore diameter of about 7.3 nm. Zhou et al. (2018) showed that biochar from waste kelp after modification with KOH contained a large number of pores with an average diameter of 200–300 nm [12].

3.3. Multi-elemental Composition of Biochars

The carbon content in raw *Cladophora glomerata* was 35.6% and it increased with the increase in temperature: for 300 °C it was 39.1%, for 350 °C—39.3%, for 400 °C—37.9% and for 450 °C—46.3%. The increase in pyrolysis temperature induced the increase in the carbon content in the biochar, which indicates high carbonization at a high pyrolysis temperature [13]. The carbon content of biochar can depend on various factors such as the type of biomass and its moisture, temperature of pyrolysis or residence time [14]. Since the type of biomass and its moisture as well as residence time were kept constant, the differences in the carbon content resulted mainly from the temperature of pyrolysis. Table 3 presents the multi-elemental composition of biochars produced at 300, 350, 400 and 450 °C.

Table 3. Multi-elemental composition of biochar.

Element	Wavelength (nm)	Biochar (mg kg^{-1} dry basis)			
		A300	A350	A400	A450
Al	308.21	133 ± 20	126 ± 19	160 ± 24	217 ± 33
Ca	315.89	13,577 ± 2715	11,654 ± 2331	14,610 ± 2922	17,977 ± 3595
Cr	267.72	4.85 ± 0.73	1.30 ± 0.19	1.90 ± 0.28	1.03 ± 0.15
Cu	324.75	4.95 ± 0.74	0.277 ± 0.042	1.15 ± 0.17	4.24 ± 0.64
Fe	259.94	471 ± 71	455 ± 68	57.0 ± 8.6	750 ± 112
K	766.49	6218 ± 1243	6435 ± 1287	7835 ± 1567	10,511 ± 2102
Mg	285.21	812 ± 122	728 ± 109	887 ± 133	1158 ± 232
Mn	257.61	182 ± 27	202 ± 30	248 ± 37	310 ± 46
Na	588.99	619 ± 93	442 ± 66	463 ± 69	705 ± 106
P	213.62	761 ± 114	752 ± 113	906 ± 136	1252 ± 250
Pb	220.35	<LOD	<LOD	<LOD	2.29 ± 0.30
Si	251.61	25.8 ± 3.9	14.5 ± 2.2	16.6 ± 2.5	6.73 ± 1.01
Zn	213.86	7.86 ± 1.18	3.28 ± 0.49	4.42 ± 0.66	8.08 ± 1.21

<LOD—below limit of detection.

Generally, the content of main macroelements—Ca, Mg, P and K—increased in the biochar with the increase in pyrolysis temperature, which overlaps with the data shown in Table 1. The ash content increased in proportion with temperature. Biochar produced from macroalgae is known to be rich in ash and inorganic nutrients including Ca, K, Mg and P [1]. Jung et al. (2016) also confirmed that with the increase in pyrolysis temperature from 200 to 800 °C, the content of Ca, K, Mg and P increased in the biochar produced from brown alga—*Undaria pinnatifida* [13].

3.4. Scanning Electron Microscopy of a Raw Alga and the Resultant Biochars

Scanning electron microscopy was employed to investigate the microstructure and morphology of the samples. This technique is quite often used for the examination of algal biochar [6,8,12,14]. SEM images of raw algal biomass and the resultant biochar produced at 450 °C (as an example) are presented in Figure 2. The silica-based structures can be easily observed over the surface and these are attributed to the diatoms within the biomass sample.
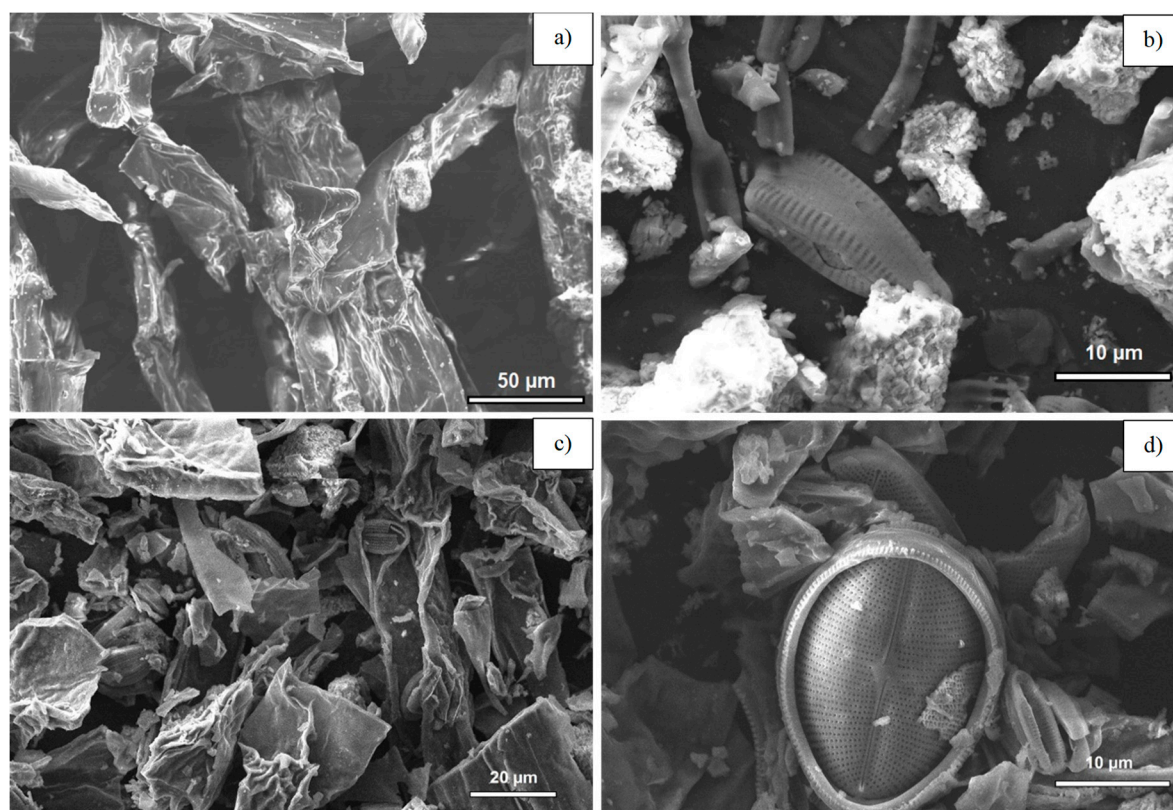
Figure 2. SEM images of (**a**,**b**) raw algae and (**c**,**d**) biochar obtained at 450 °C.

Diatoms can be found on the algal surface. The presence of diatoms is a result of convenient environmental conditions that allow their population to grow. Greenwood et al. (1999) reported the presence of diatoms over the algal surface and many species can be found in SEM images [31]. Diatoms as a component of ash remain in the biochar sample and their concentration grows along with pyrolysis temperature as their cell wall component is hydrated silicon oxide. Raw biomass appears to have a rather weakly developed surface texture in comparison to the biochar. The pores and curves on the biochar surface appear to be more developed because of the release of low-mass gaseous species during pyrolysis that might interact with solid residue (biochar). Mercury porosimetry showed that the surface area of algal biochars is rather weakly developed. Increasing temperature causes the material to agglomerate as a result of increasing ash content. Liu et al. (2019) reported that ash promotes agglomeration of biochar [32].

3.5. FT-IR Spectra of a Raw Alga and Produced Biochars

This technique compares the chemical profiles of biochar produced under different conditions (e.g., temperature), and between the raw biomass and the resulting biochar [5]. It also determines functional groups on the biochar surface that can play a key role in metal biosorption [8]. FT-IR spectra of raw *Cladophora glomerata*, apart from obtaining biochars, given in Figure 3, are typical for dried biological material. The presence of polysaccharides and proteins in the biomass was confirmed. The rise in pyrolysis temperature resulted in a significant decrease in characteristic peaks: $3500–3100$ cm^{-1} was attributed to the stretching vibrations of the O–H group [8]; $2850–2970$ cm^{-1} was assigned to the stretching vibrations of C–H bonds in aliphatic CH$_2$ and CH groups. The decreasing intensity of the peak obtained from the O–H group is an outcome of water removal, after which the material becomes more hydrophobic. Temperature rise also results in the progressing destruction of polysaccharides and peptides. For biochar A400, as seen in Figure 3, certain peaks reach their maximum in comparison to other samples: the peak at about 1605 cm^{-1} was caused by the stretching vibrations from C=C of

aromatics; the peak at 1420 cm^{-1} was attributed to the bending oscillations from CH_2 and the peak at about 1111 cm^{-1} relates to the stretching vibrations of Si–O and was due to the presence of diatoms (also observed in SEM images). The occurrence of Si–O–Si deformation vibrations was observed at 475 cm^{-1} and was also attributed to silica remaining in the biochars within the whole temperature range. The increase in silica oxide in the material is a result of the high temperature stability of this material, which is why its presence can be observed in all samples. At about 873 cm^{-1} the peak from C–H vibrations from the aromatic ring was seen. The progressing aromatization of biochar was related to the thermal conversion of lignin and other lignocellulosic compounds. At about 618 cm^{-1} there occurs the peak from Fe–O bonds.The oxygen-containing functional groups of the biomass can serve as potential biosorption sites [8]. Carboxyl and hydroxyl groups on the surface of biomass play a dominant role in the biosorption of metal ions from solutions [33,34].
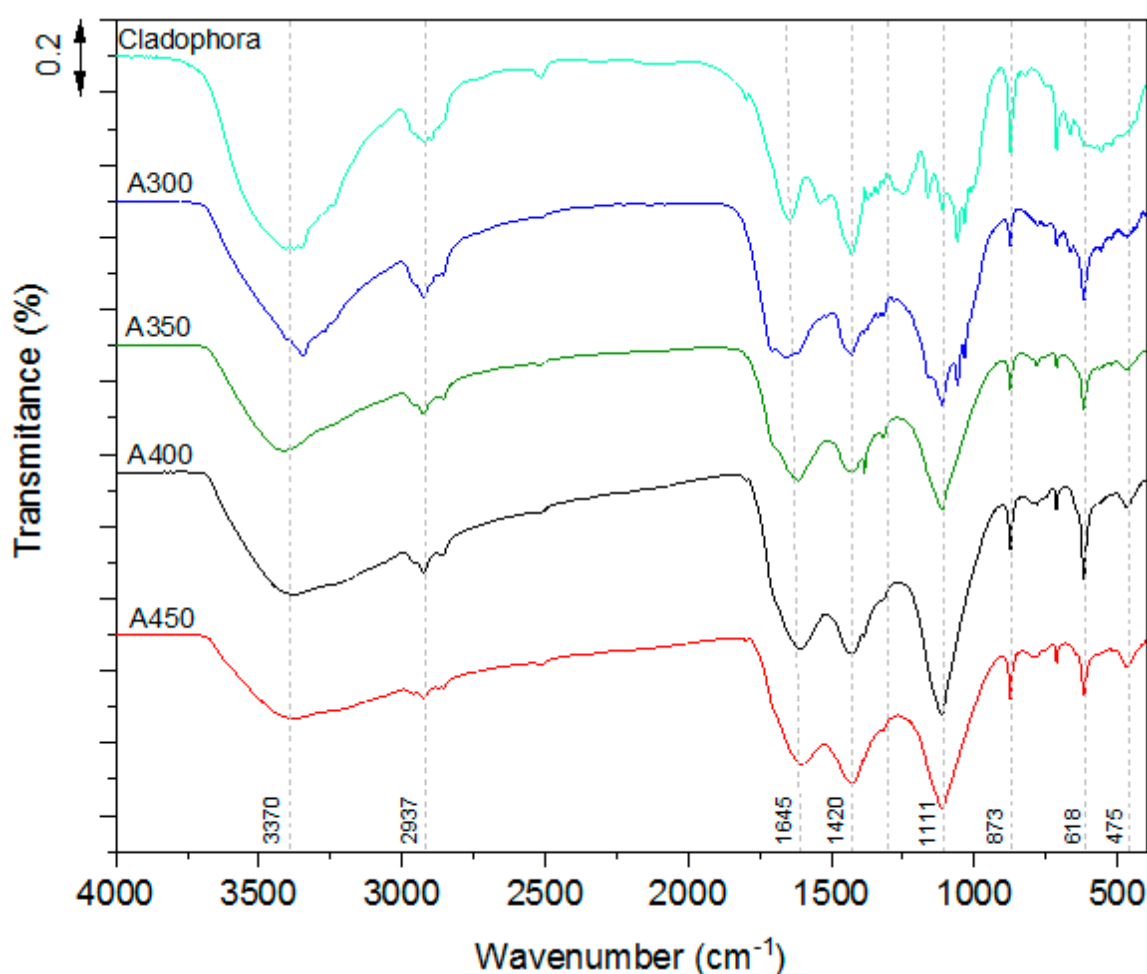
Figure 3. Fourier-transform infrared spectra of biochar formed at different temperatures.

3.6. Biosorption Properties of Biochars

Biochar is a type of porous carbon similar to activated carbon [14,30]. The surface area with the pore size and pore volume affecting its sorption characteristics [35]. We performed preliminary experiments on biosorption of Cr(III) ions by macroalgal biochars produced at different temperatures 300, 350, 400 and 450 °C. The physical and chemical properties of biochar are known to depend not only on feedstock, but also on pyrolysis temperature [36], which we found to be true.

Macroalgal biochar demonstrated very good biosorption properties, which are expressed as biosorption capacity, calculated from Equation (2):

$$q_t = \frac{(C_0 - C_t)V}{W} \tag{2}$$

where C_0 and C_t (mg L^{-1}) are the concentrations of Cr(III) ions before biosorption by biochar and at a given time t, V (L) is the volume of the solution used in biosorption experiment and W (g) is the mass of biochar in the solution.

The biosorption capacity of biochar towards Cr(III) ions increased with the increase in pyrolysis temperature (Figure 4). The equilibrium state was reached after ~80 min, so it was quite a fast process. Rapid initial sorption of metal ions has been known for quite a time [20,25,33]. Gokulan et al. (2019) showed that the sorption of dye by the biochar from green seaweed *Ulva lactuca* was rapid and occurred within the first hour, which was caused by easily available binding groups (functional groups) on biochar surface [37].
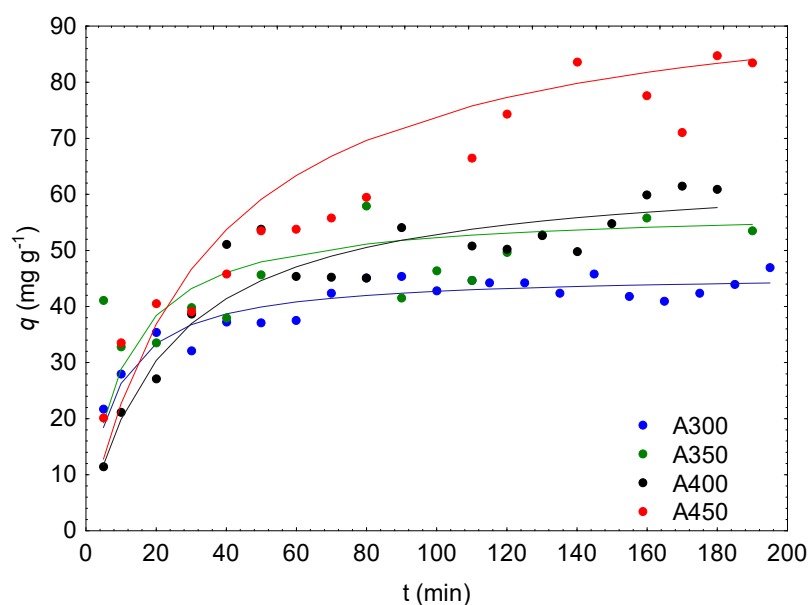
Figure 4. Kinetics of biosorption of Cr(III) ions by biochar produced at different temperatures.

The kinetics of metal ions biosorption is generally described by the pseudo-first (Equation (3)) and the pseudo-second order model (Equation (4)) [7,9,24,33,37]:

$$\frac{dq_t}{dt} = k_1 \cdot (q_{eq1} - q_t) \tag{3}$$

$$\frac{dq_t}{dt} = k_2 \cdot (q_{eq2} - q_t)^2 \tag{4}$$

where q_{eq1}, q_{eq2} and q_t are the amounts of adsorbed metal ions on the biosorbent at equilibrium and at time t (mg g^{-1}), and k_1 and k_2 are the rate constants of the pseudo-first (min^{-1}) and pseudo-second order model of biosorption (g mg^{-1} min^{-1}).

From the linear form of Equations (3), (Equation (5)) and (4) (Equation (6)) it was possible to determine the parameters of q_{eq1}, k_1, q_{eq2} and k_2, respectively:

$$\ln(q_{eq1}\text{-}q_t) = \ln(q_{eq1}) - k_1 \times t \tag{5}$$

$$\frac{t}{q_t} = \frac{1}{k_2 \cdot q_{eq2}^2} + \frac{t}{q_{eq2}} \tag{6}$$

In order to determine the mechanism of biosorption, the Weber and Morris model (1963) can be applied as in Equation (7):

$$q_t = k_p t^{0.5} + C \tag{7}$$

where k_p is the intraparticle diffusion rate constant (mg g^{-1} min$^{-0.5}$) and C is the intercept (mg g^{-1}) [38].

The best model describing the biosorption kinetics was chosen on the basis of R^2 value. Figure 5a—the example for biochar produced at 450 °C shows that the experimental data showed better comply with the proposed pseudo-second order model (R^2 0.965) than with the pseudo-first order model (R^2 0.899)—Figure 5b and the interparticle diffusion model (R^2 0.829)—Figure 5c. This is why, the parameters of the pseudo-second order model were used for the description and comparison of biosorption properties of *Cladophora glomerata* biochar. These results are in line with the data presented by Zhou et al. (2018), who used the pseudo-first and pseudo-second order model for the description of biosorption kinetics of dyes (methylene blue) by biochar produced from waste kelp. It was shown that adsorption kinetics fitted well with a pseudo-second order model [12]. It was similar in the case of the sorption of Remazol dyes by biochar from green seaweed *Ulva lactuca* [37].

(a)
t/q=0.0103 t+0.380; R^2=0.965

(b)
ln(q_{eq}-q)=-0.0088 t+4.28; R^2=0.899

Figure 5. *Cont.*

(c)
$q_t = 5.73 \cdot t^{0.5} + 12.18;\ R^2 = 0.829$
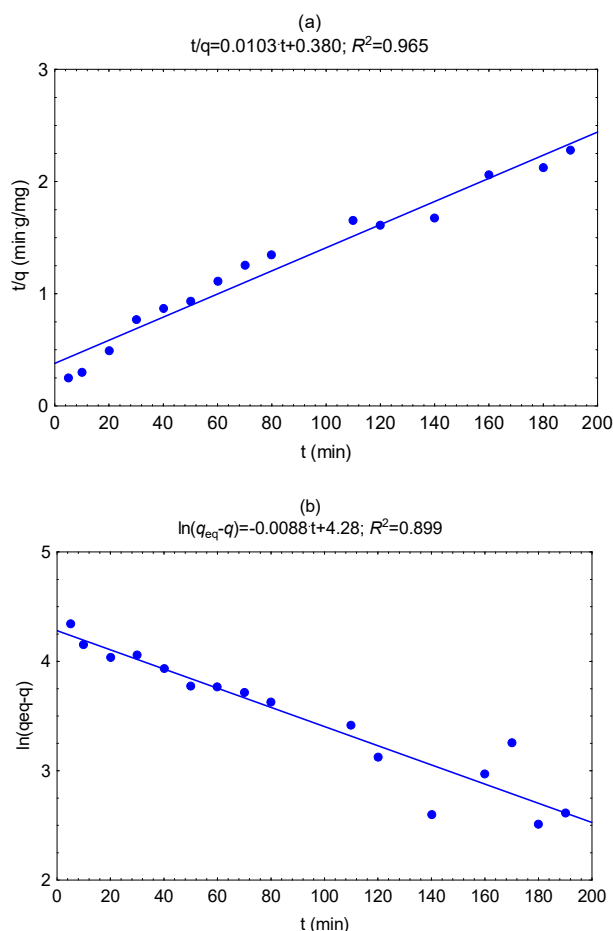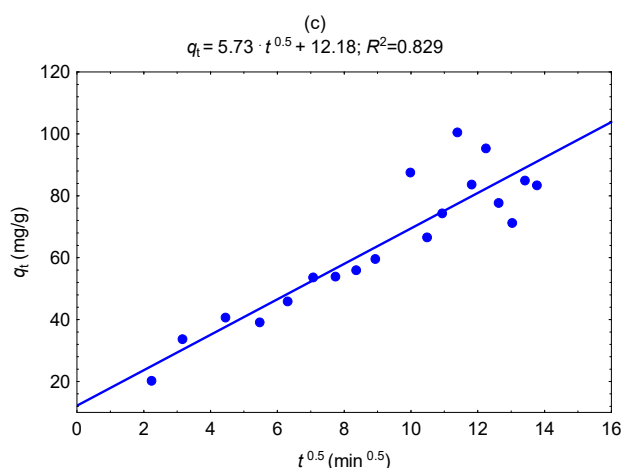
Figure 5. Kinetic plots for the biosorption of Cr(III) ions onto *Cladophora glomerata* biochar obtained at 450 °C applying different kinetic models (**a**) pseudo-second, (**b**) pseudo-first order model, (**c**) interparticle diffusion model (C_0 300 mg L^{-1}, pH 5, C_S 1 g L^{-1}, 25 °C).

The parameters of the pseudo-second order model, as well as the Weber and Morris model for the biosorption of Cr(III) ions by biochars—A300, A350, A400 and A450 are presented in Table 4.

Table 4. The parameters of the pseudo-second order model and intraparticle diffusion model for the biosorption of Cr(III) ions on biochars (C_0 300 mg L^{-1}, pH 5, C_S 1 g L^{-1}, 25 °C).

Biochar	Pseudo-second Order Model			Weber and Morris Diffusion		
	q_{eq2} (mg g^{-1})	k_2 (g mg^{-1} min^{-1})	R^2	k_p (mg g^{-1} min$^{-0.5}$)	C (mg g^{-1})	R^2
A300	45.9	0.00292	0.991	1.30	28.5	0.680
A350	57.5	0.00175	0.925	2.09	26.2	0.866
A400	64.9	0.000678	0.965	3.57	15.4	0.756
A450	87.1	0.000279	0.965	5.73	12.2	0.829

The biosorption capacity of biochar obtained at 450 °C (A450) was almost twice higher than that reached at a temperature of 300 °C: 41% higher for A400 by and 25% higher for A350. Rate constants of Cr(III) ion biosorption by biochars decreased with the increase in pyrolysis temperature. Jung et al. (2016) also observed the increase in the phosphate adsorption capacity concurrent with the increase in pyrolysis temperature of up to 400 °C. A further increase in pyrolysis temperature lowered adsorption capacity due to blocked pores in the biochar during pyrolysis [13]. It was also found that with the increase in the carbon content in biochar, biosorption capacity—q_{eq2} also increased. This relationship was also observed for biocomposites produced from different cellulosic substrates (barley husk, peanut shells and sawdust), i.e., biosorbents with a higher percentage of carbon showed higher capacities [9].

In our previous study we showed that the biosorption capacity of natural *Cladophora glomerata*, determined from the pseudo-second order model, was 78.1 mg g^{-1} (C_0 300 mg L^{-1}, pH 5, C_S 1 g L^{-1}, 25 °C) [25], which is smaller than the biosorption capacity of biochar obtained from this alga at 450 °C. The biosorption capacity of A450 was by 11% higher than for the raw biomass. Kidgell et al. (2014) also demonstrated that the biochar produced from the freshwater macroalga *Oedogonium* sp. (*Chlorophyta*) was the most effective biosorbent among other tested such as dried biomass and Fe-treated biomass, removing metals (including Al, Cd, Cr, Cu, Mn, Ni, Pb and Zn) from complex industrial effluent from a coal-fired power station [20].

The application of the Weber and Morris model to the experimental data enabled to determine whether the adsorption process was governed only by intraparticle diffusion, or it was more complex and the biosorption occurred due to surface adsorption, ion exchange, complexation, chelation or microprecipitation [10]. When the intercept—C (which is associated with the thickness of the boundary layer) equals zero, then the intraparticle diffusion is the only controlling step [10,38]. In the case of

biosorption of Cr(III) ions by biochars, *C* was higher than zero, and it decreased with the increase of temperature of biochar production. In this study, *C* does not pass through the origin what indicates that there are other processes involved in the rate of adsorption [10]. The parameter k_p illustrates an enhanced rate of adsorption [39]. In our study, k_p increased with an increase of biomass pyrolysis temperature. Larger k_p values show better adsorption which is related to improved binding between the metal ions in the solution (sorbate) and biochar (biosorbent) [39].

The biosorption properties of bioachar obtained at 450 °C were also tested in a multi-metal system with artificial wastewater that contained Cu(II), Zn(II) and Cr(III) ions. The ability to simultaneously remove multiple metal ions from polluted solutions makes biochar a very successful biosorbent in a multi-elemental context [20]. Our results are presented in Table 5.

Table 5. The multi-elemental composition of the wastewater before and after biosorption with biochar—A450 (pH 5, C_S 1 g L^{-1}, 25 °C).

Element	Wavelength (nm)	Concentration of Metal Ions (mg L^{-1}) in Wastewater:	
		Before Biosorption	After Biosorption
Ca	315.89	<LOD	10.8 ± 1.6
Cr	267.72	1.02 ± 0.15	0.104 ± 0.016
Cu	324.75	0.412 ± 0.062	0.014 ± 0.003
K	766.49	1.67 ± 0.25	29.7 ± 4.5
Mg	285.21	<LOD	1.57 ± 0.24
Na	588.99	6.18 ± 0.93	7.38 ± 1.11
Zn	213.85	3.72 ± 0.56	0.234 ± 0.035

<LOD—below limit of detection.

The removal efficiency (*R*; %) calculated from Equation (8), for Cr(III), Cu(II) and Zn(II) ions was as follows: 89.9%, 97.1% and 93.7%.

$$R = \frac{C_0 - C_t}{C_0} \times 100\% \tag{8}$$

In the work of Kidgell et al. (2014), it was shown that the biochar produced from freshwater macroalga *Oedogonium* at 450 °C had a satisfactory removal efficiency of Cr(III), Cu(II) and Zn(II) ions from industrial effluent from a coal-fired power station. For Cr(III) ions it was 50%, Cu(II) ions—37% and for Zn(II) ions—92% [20]. Thivya and Vijayaraghavan (2019) reported that red seaweed-derived biochar (obtained from *Kappaphycus alvarezii* at 350 °C) was also efficient in the removal of reactive dyes, such as reactive orange 16 and reactive blue 4 in mono- and binary-contaminated waters [40]. Gokulan et al. (2019) demonstrated the potential of biochar synthesized from green seaweed *Ulva lactuca* at 300 °C to remove Remazol dyes from complex dye wastewaters. The dye removal efficiency was above 77.5% [37]. Therefore, biosorption with macroalgae-based products can be recognized as a promising technology for the bioremediation of industrial effluents. In comparison with classical adsorbents such as activated carbon, silica or alumina gel, renewable resources such as waste macroalgae or lignocellulosic residues appear as an eco-friendly alternative to the efficient removal of contaminants from industrial wastewater [10,11].

We observed that the content of light metal ions (Ca, K, Mg, Na) in the solution after biosorption increased (especially K), which indicates that ion-exchange played a major role in this process [18,20]. This is in line with the results obtained from the Weber and Morris model. The mechanisms of Cr(III) ion adsorption on macroalgal biochar pyrolyzed at different temperatures should be further studied.

4. Conclusions

We have experimented with the production of biochar from freshwater macroalga *Cladophora glomerata*. The yield of pyrolysis increased an increase in temperature and was at the highest at 450 °C—47%. All biochars were characterized by a similar total pore area which was about 20 m² g^{-1}. SEM analysis showed small pores on the sample surface. FT-IR data indicated the participation of

O-H, Si–O, –CH, –CH$_2$ groups in Cr(III) removal by the algal biochar. We have also shown that *Cladophora glomerata* biochar has a great potential as a renewable adsorbent to remove toxic metals from wastewaters. The biosorption capacity of algal biochar towards Cr(III) ions increased with the increase in pyrolysis temperature and the best results were obtained for biochar produced at 450°C—87.1 mg g^{-1}. *Cladophora* biochar demonstrated also a good ability to simultaneously remove metal ions from artificial wastewater. The removal efficiency for Cr(III) was 89.9%, for Cu(II)—97.1% and for Zn(II) ions—93.7%. Thus, biochar derived from *Cladophora glomerata* can be used as a cost-effective and efficient adsorbent for the removal of metal ions from aqueous solutions. Further research on biosorption equilibrium and process mechanism are required.

References

1. Bird, M.; Wurster, C.M.; de Paula Silva, P.H.; Bass, A.M.; de Nys, R. Algal biochar—production and properties. *Bioresour. Technol.* **2011**, *102*, 1886–1891. [CrossRef] [PubMed]

2. Mihranyan, A. Cellulose from *Cladophorales* green algae: From environmental problem to high-tech composite materials. *J. Appl. Polymer Sci.* **2011**, *119*, 2449–2460. [CrossRef]

3. Torres, M.D.; Kraan, S.; Domínguez, H. Seaweed biorefinery. *Rev. Environ. Sci. Bio/Technol.* **2019**, *18*, 335–388. [CrossRef]

4. Chaiwong, K.; Kiatsiriroat, T.; Vorayos, N.; Thararax, C. Biochar production from freshwater algae by slow pyrolysis. *Maejo Int. J. Sci. Technol.* **2012**, *6*, 186–195.

5. Yu, K.L.; Lau, B.F.; Show, P.L.; Ong, H.C.; Ling, T.C.; Chen, W.H.; Ng, E.P.; Chang, J.S. Recent developments on algal biochar production and characterization. *Bioresour. Technol.* **2017**, *246*, 2–11. [CrossRef] [PubMed]

6. Poo, K.M.; Son, E.B.; Chan, J.S.; Ren, X.H.; Choi, Y.J.; Chae, K.J. Biochars derived from wasted marine macro-algae (*Saccharina japonica* and *Sargassum fusiforme*) and their potential for heavy metal removal in aqueous solution. *J. Environ. Manag.* **2018**, *206*, 364–372. [CrossRef] [PubMed]

7. Laird, D.A.; Brown, R.C.; Amonette, J.E.; Lehmann, J. Review of the pyrolysis platform for coproducing bio-oil and biochar. *Biofuels Bioprod. Biorefin.* **2009**, *3*, 547–562. [CrossRef]

8. Son, E.B.; Poo, K.M.; Chang, J.S.; Chae, K.J. Heavy metal removal from aqueous solutions using engineered magnetic biochars derived from waste marine macro-algal biomass. *Sci. Total Environ.* **2018**, *615*, 161–168. [CrossRef]

9. Perez-Ameneiro, M.; Bustos, G.; Vecino, X.; Barbosa-Pereira, L.; Cruz, J.M.; Moldes, A.B. Heterogenous lignocellulosic composites as bio-based adsorbents for wastewater dye removal: A kinetic comparison. *Water Air Soil Pollut.* **2015**, *226*, 133. [CrossRef]

10. Vecino, X.; Devesa-Rey, R.; Villagrasa, S.; Cruz, J.M.; Moldes, A.B. Kinetic and morphology study of alginate-vineyard pruning waste biocomposite vs. non modified vineyard pruning waste for dye removal. *J. Environ. Sci.* **2015**, *38*, 158–167. [CrossRef]

11. Cutillas-Barreiro, L.; Paradelo, R.; Igrexas-Soto, A.; Nunez-Delgado, A.; Fernandez-Sanjurjo, M.J.; Alvarez-Rodriguez, E.; Garrote, G.; Novoa-Munoz, J.C.; Arias-Estevez, M. Valorization of biosorbent obtained from a forestry waste: Competitive adsorption, desorption and transport of Cd, Cu, Ni, Pb and Zn. *Ecotox. Environ. Saf.* **2016**, *131*, 118–126. [CrossRef] [PubMed]

12. Zhou, Y.; Zhang, H.; Cai, L.; Guo, J.; Wang, Y.; Ji, L.; Song, W. Preparation and characterization of macroalgae biochar nanomaterials with highly efficient adsorption and photodegradation ability. *Materials* **2018**, *11*, 1709. [CrossRef] [PubMed]

13. Jung, K.W.; Kim, K.; Jeong, T.U.; Ahn, K.H. Influence of pyrolysis temperature on characteristics and phosphate adsorption capability of biochar derived from waste-marine macroalgae (*Undaria pinnatifida* roots). *Bioresour. Technol.* **2016**, *200*, 1024–1028. [CrossRef] [PubMed]

14. De Bhowmick, G.; Sarmah, A.K.; Sen, R. Production and characterization of a value added biochar mix using seaweed, rice husk and pine sawdust: A parametric study. *J. Cleaner Prod.* **2018**, *200*, 641–656. [CrossRef]

15. Cole, A.J.; Paul, N.A.; de Nys, R.; Roberts, D.A. Good for sewage treatment and good for agriculture: Algal based compost and biochar. *J. Environ. Manag.* **2017**, *200*, 105–113. [CrossRef] [PubMed]

16. De Ramon N'Yeurt, A.; Iese, V. The proliferating brown alga *Sargassum polycystum* in Tuvalu South Pacific: Assessment of the bloom and applications to local agriculture and sustainable energy. *J. Appl. Phycol.* **2015**, *27*, 2037–2045. [CrossRef]

17. Kiran, H. Application of biochar technologies to wastewater treatment. Ph.D Thesis, Massey University, Palmerston North, New Zealand, 2013. Available online: https://muir.massey.ac.nz/bitstream/handle/10179/4288/02_whole.pdf (accessed on 21 September 2017).

18. Davis, T.A.; Volesky, B.; Mucci, A. A review of the biochemistry of heavy metal biosorption by brown algae. *Water Res.* **2003**, *37*, 4311–4330. [CrossRef]

19. Jiang, Y.; Lei, M.; Duan, L.; Longhurst, P. Integrating phytoremediation with biomass valorisation and critical element recovery: A UK contaminated land perspective. *Biomass Bioenerg.* **2015**, *83*, 328–339. [CrossRef]

20. Kidgell, J.T.; de Nys, R.; Hu, Y.; Paul, N.A.; Roberts, D.A. Bioremediation of a complex industrial effluent by biosorbents derived from freshwater macroalgae. *PLoS ONE* **2014**, *9*, e94706. [CrossRef]

21. Johansson, C.L.; Paul, N.A.; de Nys, R.; Roberts, D.A. Simultaneous biosorption of selenium, arsenic and molybdenum with modified algal-based biochars. *J. Environ. Manag.* **2016**, *165*, 117–123. [CrossRef]

22. Starmach, K. *Family: Cladophora Kutzing 1843. Identification Key*; Freshwater Biological Association: Windermere, UK, 1975.

23. Ni, Y.; Chen, S.; Kokot, S. Spectrophotometric determination of metal ions in electroplating solutions in the presence of EDTA with the aid of multivariate calibration and artificial neural networks. *Anal. Chim. Acta* **2002**, *463*, 305–316. [CrossRef]

24. Michalak, I.; Chojnacka, K. The new application of biosorption properties of *Enteromorpha prolifera*. *Appl. Biochem. Biotechnol.* **2010**, *160*, 1540–1556. [CrossRef] [PubMed]

25. Godlewska, K.; Marycz, K.; Michalak, I. Freshwater green macroalgae as a biosorbent of Cr(III) ions. *Open Chem.* **2018**, *16*, 689–701. [CrossRef]

26. *Order of the Minister of Environment of November 18, 2014 laying down conditions for the introduction of sewage into Water Bodies or Soil and Laying Down the List of Substances Particularly Harmful to Water Environments, J. Laws No. 2014 Item 1800. [Rozporządzenie Ministra Środowiska z dnia 18 listopada 2014 r. w Sprawie Warunków, Jakie Należy Spełnić Przy Wprowadzaniu Ścieków do Wód Lub do Ziemi, Oraz w Sprawie Substancji Szczególnie Szkodliwych dla Środowiska Wodnego, Dz.U. 2014 poz. 1800]*; Internetowy System Aktów Prawnych: Warsaw, Poland, 2014.

27. *Solid Biofuels. Determination of Moisture Content. Oven Dry Method. Part 2: Total Moisture. Simplified Method*; PN-EN ISO 18134-2:2017-03; The Polish Committee for Standardization (Polski Komitet Normalizacyjny—PKN): Warszawa, Poland, 2017.

28. *Solid Mineral Fuels. Determination of Ash*; PN-ISO 1171:2002; The Polish Committee for Standardization (Polski Komitet Normalizacyjny—PKN): Warszawa, Poland, 2002.

29. *Solid Biofuels. Determination of The Content of Volatile Matter*; PN-EN ISO 18123:2016-01; The Polish Committee for Standardization (Polski Komitet Normalizacyjny—PKN): Warszawa, Poland, 2018.

30. Wang, H.; Zhang, M.; Lv, Q. Removal efficiency and mechanism of Cr(VI) from aqueous solution by maize straw biochars derived at different pyrolysis temperatures. *Water* **2019**, *11*, 781. [CrossRef]

31. Greenwood, J.L.; Clason, T.A.; Lowe, R.L.; Belanger, S.E. Examination of endopelic and epilithic algal community structure employing scanning electron microscopy. *Freshwater Biol.* **1999**, *41*, 821–828. [CrossRef]

32. Liu, H.; Chen, Y.; Yang, H.; Gentili, F.G.; Söderlind, U.; Wang, X.; Zhang, W.; Chen, H. Hydrothermal carbonization of natural microalgae containing a high ash content. *Fuel* **2019**, *249*, 441–448. [CrossRef]

33. Michalak, I.; Chojnacka, K.; Witek-Krowiak, A. State of the art for the biosorption process—a review. *Appl. Biochem. Biotechnol.* **2013**, *170*, 1389–1416. [CrossRef] [PubMed]

34. Michalak, I.; Mironiuk, M.; Marycz, K. A comprehensive analysis of biosorption of metal ions by macroalgae using ICP-OES, SEM-EDX and FTIR techniques. *PLoS ONE* **2018**, *13*, e0205590. [CrossRef]

35. Gai, X.; Wang, H.; Liu, J.; Zhai, L.; Liu, S.; Ren, T.; Liu, H. Effects of feedstock and pyrolysis temperature on biochar adsorption of ammonium and nitrate. *PLoS ONE* **2014**. [CrossRef]

36. Luo, L.; Xu, C.; Chen, Z.; Zhang, S. Properties of biomass-derived biochars: Combined effects of operating conditions and biomass types. *Bioresour. Technol.* **2015**, *192*, 83–89. [CrossRef]

37. Gokulan, R.; Prabhu, G.G.; Jegan, J. Remediation of complex remazol effluent using biochar derived from green seaweed biomass. *Int. J. Phytoremed.* **2019**. [CrossRef] [PubMed]

38. Weber, W.J.; Morris, J.C. Kinetic of adsorption on carbon from solutions. *J. Sanit. Eng. Div. ASCE* **1963**, *89*, 31–60.

39. Erhan, D.; Kobya, M.; Ehf, S.; Ozkan, T. Adsorption kinetics for Cr (VI) removal from aqueous solution on activated carbon prepared from Agro wastes. *J. Water* **2004**, *30*, 533–541.

40. Thivya, J.; Vijayaraghavan, J. Single and binary sorption of reactive dyes onto red seaweed-derived biochar: Multi-component isotherm and modelling. *Desal. Water Treat.* **2019**, *156*, 87–95. [CrossRef]